Proceedings World Geothermal Congress 2010
Bali, Indonesia, 25-29 April 2010

Integration of Surface and Well Data to Determine Structural Controls on Permeability at Salak (Awibengkok), Indonesia

Jim Stimac, Marino Baroek, Aquardi Suminar, and Birean Sagala

Sentral Senayan II Office Tower, 26th Fl, Jl. Asia Afrika No. 8, Jakarta 10270, Indonesia

jstimac@chevron.com

Keywords: Awibengkok, Salak, permeability, well data, surface mapping, structure, volcanic vents, intrusion.

ABSTRACT

The hot fluid upflow at Awibengkok (Salak) appears to be controlled by deep intrusion along the general E-W trend of the Sunda Volcanic Arc. At shallow levels of the geothermal system the hot fluid upflow is localized along N- to NE-trending faults and fractures where subvolcanic intrusions (small stocks, dikes, sills) may be found closest to the surface. The NNE-trending Awi fault, which controls the locations of recent volcanic vents, plays an important role in segmenting the system, and allowing the descent of shallow fluids into the eastern portion of the geothermal reservoir. Similarly, the NNE-striking Gagak fault forms an important compartment boundary on the west. Together these structures bound a zone of extension, recent volcanism and subsidence that hosts a thicker and more permeable volcanic pile than the adjacent areas.

Surface and subsurface fault and fracture patterns, determined from photo lineament interpretation, geologic mapping, and formation image logs indicate strongly anisotropic permeability aligned with the dominant N to NE fracture trend, dividing the field into a number of subcompartments that are locally connected by fractured aquifers and NW- and E-W-trending fractures. The local maximum principal stress is vertical, whereas the maximum horizontal stress is oriented approximately N-S to NNE. These structural trends are consistent with open fractures being optimally oriented relative to an approximately E-W minimum stress direction.

Subsurface offsets on the Rhyodacite Marker (RDM) and basement rocks serve as the main basis for interpretation of reservoir structure. A structural map of the field on the top of the RDM unit shows a fault pattern that includes roughly N-S-, NE-, E-W-, and NW-trending structures, similar to that expressed by surface faults. The wide variety of evidences used to make this interpretation makes it likely that both active and inactive faults are represented.

Interpretation of open to partially open fractures trends observed in borehole image logs also indicate multiple fracture sets, with N to NE fractures most common. However some wells also have prominent NNW to N, and NE to E-W trends. Most fractures are steeply dipping to vertical. Tracer return patterns also indicate preferential N to NNE fluid flow along this open fracture trend, along the strike of optimally oriented major faults or distributed fractures, or both. However well interference tests and pressure trends also indicate semi-permeable barriers compartmentalize the reservoir and define its western margin along this same trend.

Initial-state temperatures and fluid chemical trends suggest that intersections of N to NE- and NW- or E-W trending faults facilitate fluid migration between adjacent compartments, especially along the southern and northern margins of the proven reservoir; however, these flowpaths were not validated by tracer returns. This may be because these faults represent sources of external recharge or, have relatively lower permeability than N-to-NE structures due to their unfavorable orientation within the present stress regime.

There is also evidence based on entry distributions in wells that certain stratigraphic units, such as the RDM, and their contacts act as fractured aquifers or barriers to vertical fluid flow. Fractured aquifers appear to channel fluids laterally, and link to major fault-controlled pathways. Another prominent cluster of fluid entries is associated with the contact between the Lower Volcanic Formation and the underlying marine sedimentary package. This may be related to fractures developed in or enhanced at the top of the eroded basement rocks. Contact zones between sedimentary rocks and intrusions also commonly host permeability at the deepest levels of the system.

1. INTRODUCTION

The Salak (Awibengkok) geothermal field is located in West Java along the Sunda Volcanic Arc (Fig. 1). The geothermal reservoir is associated with young volcanism and intrusion in a highland area west of the Gunung Salak stratocone and east of the Cianten caldera (Stimac et al., 2008). The hot fluid upflow at Awibengkok (Salak) appears to be controlled by deep intrusion along the general E-W trend of the Sunda Volcanic Arc.

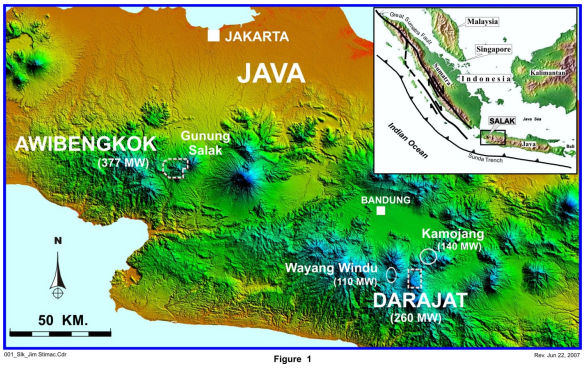

Figure 1: Topographic maps of Indonesia (top) and western Java (bottom) showing the location of the Salak (Awibengkok) geothermal area relative to nearby producing fields.

The youngest volcanic vents are concentrated along a NNE-trending Awi fault. Geologic mapping of the field and surrounding areas has improved our understanding of the distribution of volcanism and structural controls on geothermal fluid circulation. Mapping has been conducted episodically from the 1980's to present to support

development activities. Petrographic study and dating of volcanic units has provided additional constraints on the evolution of the volcanic system with time.

Downhole logging and petrographic study of cuttings and core has provided information on the stratigraphic succession and stratigraphic controls on porosity and permeability. Meanwhile leakoff tests and studies of borehole deformation and stability have provided insight into the current state of stress in the area relative to the regional trend for the volcanic arc (Sugiaman, 2003). Tracer and interference tests and monitoring of well pressure and geochemical trends over 15 years of production have provided additional information about the location of major fluid flow paths and barriers in the reservoir (Acuña et al., 2008; Stimac et al., 2008). This paper summarizes surface and subsurface evidence for structural, volcanic, and stratigraphic controls on the permeability and fluid circulation patterns in the field.

2. SURFACE STUDIES

Early geologic mapping studies of the area focused mainly on the volcanic centers, their dominant chemical composition and age (Stephenson, 1985). Faults were primarily inferred from photo lineaments and not fully integrated with interpretations of volcanic centers. The updated geologic map of the area reveals a clearer picture of the relationship between faulting and volcanism (Stimac et al., 2008). Some major unit contacts are defined by fault zones that juxtapose volcanic-sedimentary sequences of different age and composition.

2.1 Structural Trends

Figure 2 shows a simplified structural map of the area relative to topography. The NNE-trending Awi and Cibeureum faults appear to controls the locations of recent volcanic vents, playing an important role in segmenting the system, and allowing the descent of shallow fluids into the eastern portion of the geothermal reservoir (Stimac et al., 2008). To the west side of the field, the NNE-striking Gagak fault forms an important compartment boundary. It will be shown later that together these structures bound a zone of extension, recent volcanism and subsidence that hosts a thicker and more permeable volcanic pile than the adjacent areas.

The dominant strike trends of the major structures and their apparent strike length are summarized in Figure 3. It can be seen that faults striking NNW to NE (350-50°) and NW to WNW (290-310°) are dominant by length. This is consistent with these structures being the most important in terms of recent activity and effect on subsurface permeability. It will be seen below that there is evidence that these same structural trends are most important in controlling reservoir fluid flow.

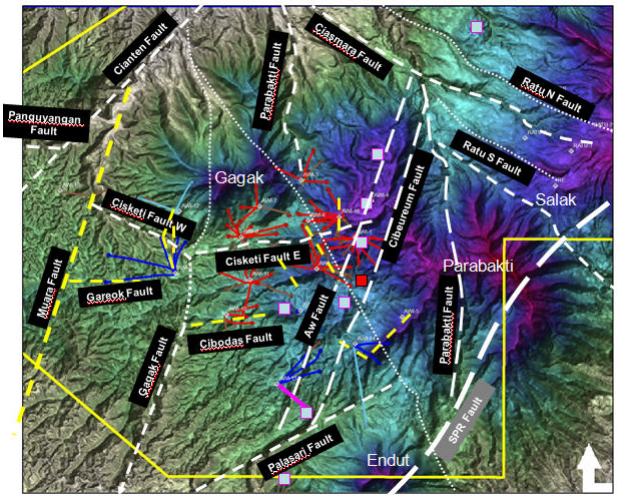

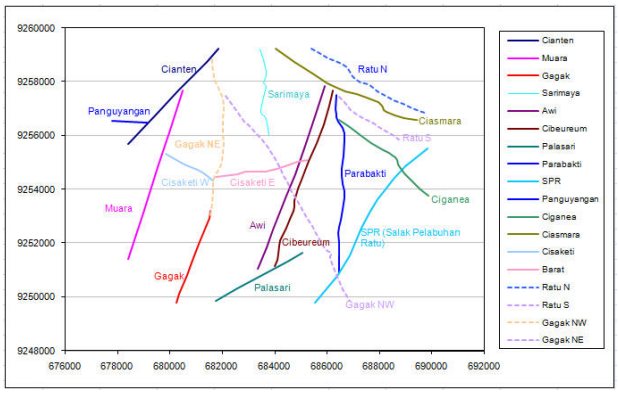

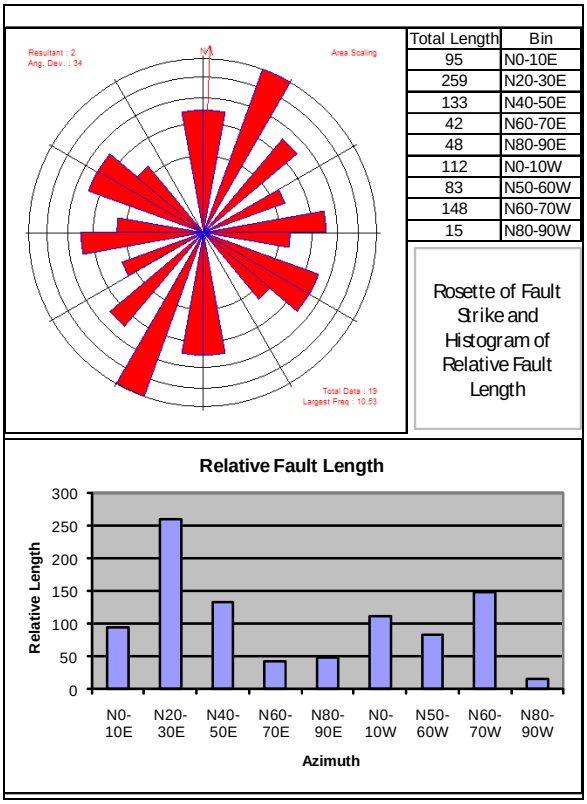

Figure 2: Map of major faults relative to topography and young volcanic vents shown as gray squares (above). The geothermal contract boundary is shown in yellow, production wells in red, and injection wells in blue and magenta. Rose diagram of fault strike and histogram of relative fault length (below).

2.1.1 Local Fault and Fractures Trends

Rose diagrams of all measured fault and fracture strikes for different areas are shown in Figure 3. Areas with older rocks show a wider range of fracture orientations, and some data may represent cooling joint rather than tectonic joints. It can be seen that fracture trends mapped within the proven reservoir boundary, where younger rocks are more prevalent generally cluster more tightly than those measured outside the area of the active geothermal system. The dominant strike trends where faults and fractures cut younger rocks are NW to NE trending, within ±40º of the regional maximum stress direction of N.

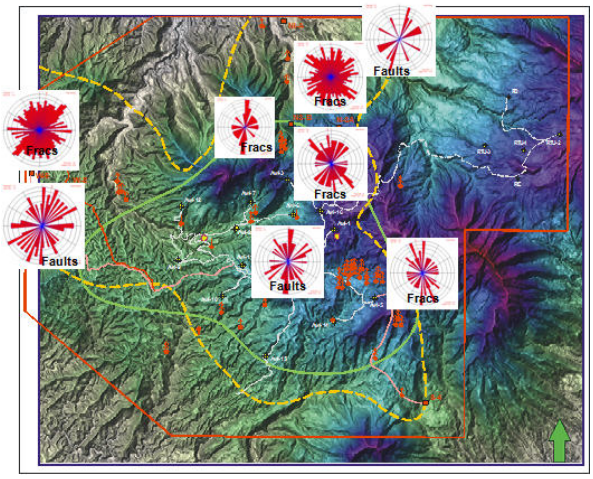

Figure 3: Strike of major faults in different portions of the study area (top).

2.1.2 Description of the Garoek Fault zone

A major E-W trending fault zones runs nearly parallel to the access road to Awi 20. This road was constructed in 2005-2006, and was mapped prior to outcrops being vegetated. It serves as an outstanding example of a mapped fault zone in the area (Figures 4 to 7). The fault zone consists of a nearly vertically trending zone that is 5 m wide and that is filled with mixed (swirled and jumbled) sheared and broken formations. The surface formations are clay-altered tuffs that do not maintain open fractures. The oldest tuffs are bedded red-brown deposits that are collectively called the Lower Brown Tuff, whereas the youngest units are the Orange Tuff and a thin overlying brown ashy soil. Apparent offset on the Orange Tuff (age estimated at 8,400 to 40,000 years based on C-14 ages on overlying and underlying units) on opposite sides of the road suggest the fault is down-to-the-north. A dip of about 75° would make this a normal fault. Subtle changes in the bed dip at the fault margin may be interpreted as drag folds with the same sense of motion. However, no slickensides or hydrothermal alteration were observed in the fault zone or at its margins. This zone dips too steeply to represent a paleostream channel. It is most likely to represent a young (<40,000 year old) fault with normal or oblique-normal slip.

Figure 4. A view of the nearly vertical E-W trending Garoek fault zone looking to the west. The fault cuts layered brown and reddish-brown tuffs that underlie the Orange Tuff and regionally extensive fallout deposit (Stimac et al., 2008). The fault zone itself is a breccia, consisting of jumbled fragments of the major tuff units it cuts. Tuff bed on opposite sides of the zone are part of the same rock sequence but show different dips and bed characteristics, and cannot be easily matched to estimate displacement.

Figure 5. The Garoek fault zone (left side of photo) and contact with bedded tuffs viewed looking S. Small subsidiary NE-striking faults cut beds at lower right.

Numerous, mostly N to NE-trending, small-displacement subsidiary faults are present near the main fault (Figures 5 and 7). Additional faults are observed near the location where the E-W fault is projected to cut the next bend in the road. NE-trending faults and breccia zones at this location are pictured in Figure 7.

Figure 6. View along the Gareok fault as seen from above and looking to the E. A large area of disrupted Orange Tuff and Upper Brown tuff can be seen from this perspective, as well as a small valley that may be controlled by the fault. Fig. 7 is a close up of the lower right at road level.

Figure 7. Subsidiary NE-trending fault and breccia zone on the W side of the Garoek fault. Note disrupted beds of Upper Brown tuff on the lower bench and Orange and Upper Brown tuff on the upper bench of the road cut.

3. SUBSURFACE STUDIES

The abundance of thick dacite and rhyolite tuff sequences in the subsurface suggests that one or more buried calderas area present in the area. Intrusion appears to be more widespread, especially in the Miocene sedimentary sequence that underlies the Pliocene to Quaternary volcanic pile, but the age of the various intrusive bodies intersected in deep wells has not been determined.

3.1 Stratigraphy and Volcanic Evolution

A detailed description of the surface stratigraphy of the Salak area can be found in Stimac et al. (2008). In this paper we focus on key rock units that appear to influence the permeability characteristics of the geothermal system. The Rhyodacite Marker, a thick sequence of silicic tuffs, is present at -300 to -1600 ft asl throughout the field. Many of the fluid entries in the reservoir are located within this unit, and where it is intersected in injection wells, nearby producers show cooling trends in the same unit.

Another horizon of abundant fluid entries is present on the west side of the field near the contacts of a mixed volcanic and sedimentary sequence. These rocks were deposited in a shallow marine setting in Miocene time. They also outcrop along the south coast of west Java, where they have been folded and thrust-faulted. Uplift prior to the more recent episodes of volcanism, may have enhanced permeability along former erosional surfaces on this unit.

3.2 Structural Trends

Borehole image logs and core samples provide the best evidence regarding the orientation of open fractures in the reservoir. Most core samples that have been obtained have not been oriented, but paleomagnetic studies have allowed reorientation of a few samples. In other core samples, the characteristics of fractures, including dip, spacing, amount of open space and mineral sealing, and the paragenesis of mineral fillings have been studied (Moore and Norman, 1999; Hulen et al., 1999).

3.2.1 Detailed Fracture Trends in Awi 1-2 Corehole

The near-vertical Awi 1-2 corehole provides about 3000 ft of continuous core samples through the steam cap and liquid zone of the eastern reservoir. Core provides "groundtruth" to calibrate the image log interpretation, giving a clearer understanding of the characteristics of the fracture network, including dip angle, amount of open space, and mineral fillings. An abundance of sealed fractures and sealed hydrothermal breccias have been described relative to open space (Hulen et al., 1999), and based on evidence of abundant sealed veins and breccias in other cores and borehole image logs, this is believed to be typical of the hydrothermal fracture network in general.

Comparing fracture interpretations derived from core and image logs is instructive. Core and image log derived dip trends for Awi 1-2 are similar but have some minor systematic differences. Near-vertical fractures are clearer in core than in image logs, where they may be missed or mistaken for induced fractures (Figure 8 and 9). Similarly low angle fractures appear to have been partially interpreted as bedding in the log. Statistical treatment of the fracture population provides a way to input fracture trends to simulation models (Figure 9). The vast majority of open fractures observed in core are steeply dipping. In Awi 1-2, 65% of fractures dip ≥60° and 87% dip ≥40°.

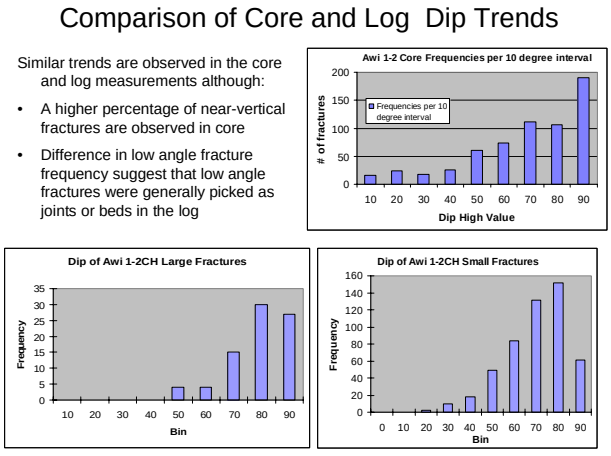

Figure 8: Histogram of open fracture dip from Awi 1-2 well from core (upper right) and image log (lower).

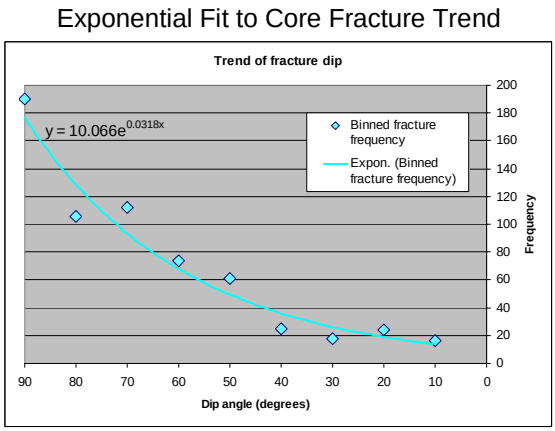

Figure 9: Exponential fit to trend from Figure 8.

3.2.2 Fieldwide Fracture Trends from Borehole Image Logs

Borehole image logs were used to interpret geological features such as rock type, bedding, and natural and induced fractures. Fracture orientation (dip, dip azimuth) is determined from picking and matching sinusoids to fracture traces on the log. Fractures in geothermal samples may be planar, curvilinear, complexly branching, or define stockworks (multiple overlapping fracture sets), thus not all sealed fractures observed in core can be identified and mapped during log interpretation. Moreover comparison of core and logs from the same interval reveal that not all sealed and partial sealed fractures seen in core are visible on image logs.

Natural fractures that could be identified in logs were classified as open, partially open, sealed depending on whether the sinusoid was visible on all pads and partially to completely filled by conductive fluid. Fractures that were partially filled by more resistive minerals relative to the matrix, or were only convincingly defined on 2 or 3 pads, were interpreted as partially open. Sinusoids that appeared to be composed of resistive minerals were considered sealed. Fractures with evidence of offset were interpreted as faults. Some examples of open, partially open and sealed fractures are shown in Figures 10 to 13.

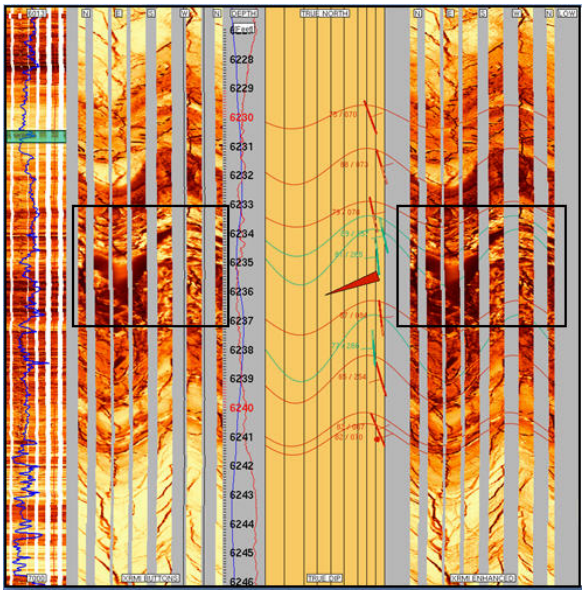

Figure 10: Awi 19-2OH XRMI log (6233-6637'). An example of a steeply dipping sealed fracture (vein) in black box (dip pick in red, resistive, light colored) with some open space (dip picks in green, conductive, dark colored) along its bottom face. Host rock is a lava flow unit (resistive).

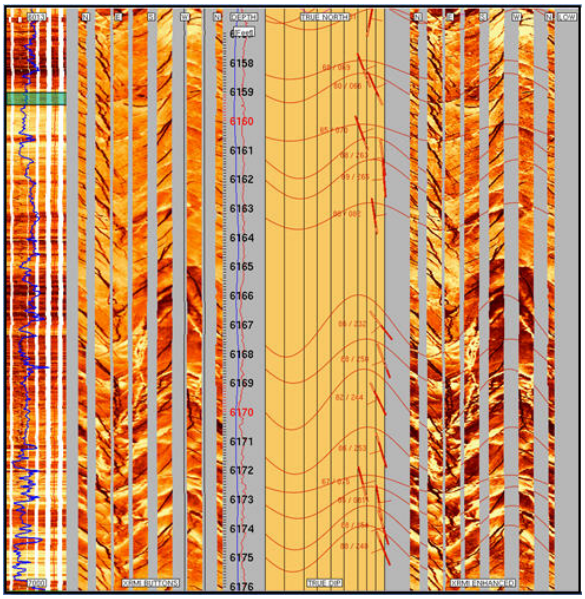

Figure 11: Awi 19-2OH XRMI log (4554-4556') showing numerous sealed fractures (dip picks in red, resistive) cutting a moderately resistive lava flow unit.

Fractures formed during the drilling process were classified as tensile fractures or borehole breakouts, but are not described in detail. These features are typically visible on two pads at 90° angles and run along the borehole wall. In geothermal wells tensile fractures are much more common than borehole breakouts because of the large magnitude of tensile forces induced by cooling of the borehole during drilling. Irregular NE-SW tensile fractures can be seen in most of the Figures shown in well Awi 19-2.

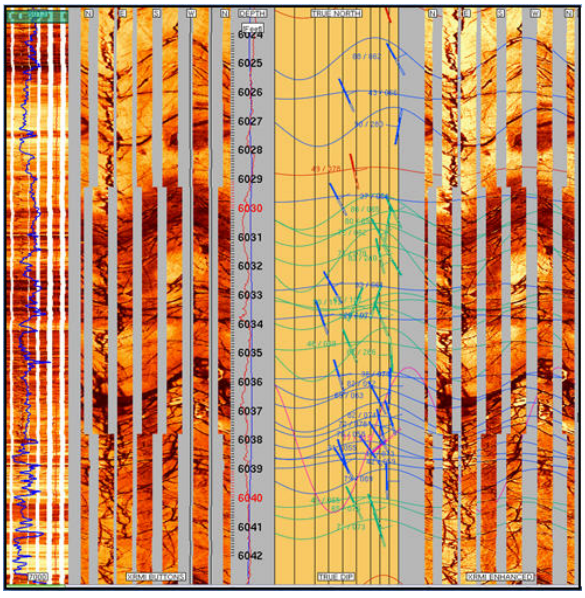

Figure 12: Awi 19-2OH XRMI LOG (6024-6041') with numerous partially (green) to open (blue) fractures

NNW to N-striking fractures within and highly resistive lava flow unit.

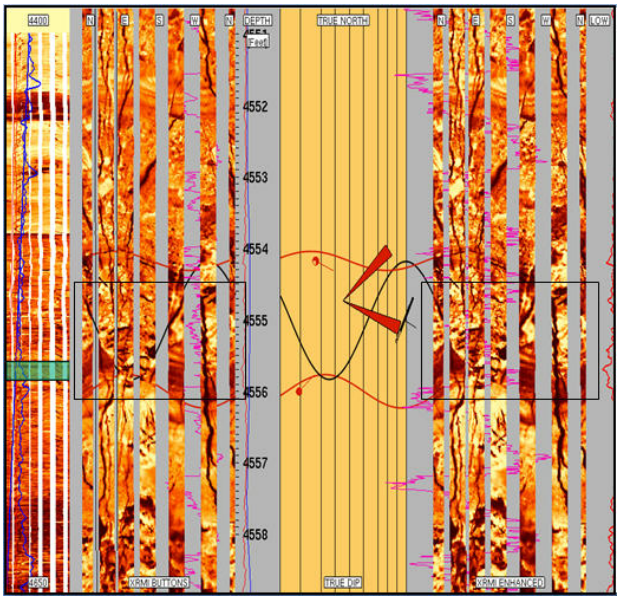

Figure 13: Awi 19-2OH XRMI LOG (4554-4556') showing a small open NE-striking fault (black, in box).

Next we describe the observed strike trends of open to partially open fractures throughout the Salak field (Figure 14). Orientations of these geological features were analyzed with regard to known well entries from pressure-temperature-spinner logs, and the broader fracture and fault patterns of the field determined from other data. It was found that only a small fraction of the fractures that were mapped as open or partially open actually support measureable fluid flow. Based on core studies, this is likely because most fractures contain mineral and breccia fillings along their strike that tend to eventually isolate them. Thus vuggy open space may be seen at a particular location along strike even if the fracture is blocked at some other location.

The dominant strike of fractures determined from image logs is N to NE, in agreement with the dominant fracture pattern in Salak field from surface data. However in detail, multiple fracture sets are apparent, especially in some wells on the periphery of the proven reservoir. Moreover trends change with depth in some wells (e.g., Awi 18-1 as shown in Yoshioka and Stimac, 2010).

Several trends in well fracture patterns can be identified:

1) A dominant group with a N-NNE (0-20^o) striking fracture trend was found in the central and eastern parts of the Salak field.

2) A second group with a N-NNE (0-20^o) striking fracture trend, associated with ENE to E-W (70-90^o) and NW (300-330^o) striking fracture trends. This group mostly located in west of Salak field.

3) The third group with a N-NNW (340-350^o) trend, associated with a N striking fracture trend which is identified near to the reservoir boundary.

These well groups show fracture patterns similar with major faults develop near and/or intersecting them with the exception to the third group. Wells with the N-NE fracture trend are located near or intersecting the N-NNE Awi fault and/or Cibereum fault (Awi 1-2, 1-8, 16-1, 2-2, and 19-3). Meanwhile the second group is found in wells that were drilled intersecting and/or close N-NE Gagak Fault and Cianten Fault; E-W Cisaketi fault.

The similarity between the strike of open fracture and strike of nearby faults suggests that open fractures are strongly associated with faults. Fault and related fractures act as pathways for fluid parallel to the strike direction of these structures. It shows that in the central and eastern parts of the Salak field, the N-NE Awi and Cibereum faults dominate are strongly mirrored in open fracture trends. Meanwhile in west Salak, multiple open fracture sets reflect the more complex fault pattern. The E-W trending Garoek and Cisaketi faults are mirrored by the E-W open fracture set prominent in Awi 20 and Awi 9 wells. It can be seen in Figure 14 that the forked leg (FL) of Awi 20-1 cuts the Garoek fault and has a significantly higher portion of E-W open fractures than the original hole (OH).

The N-NW fracture trend which was observed in wells drilled near the reservoir boundary (Awi 19-2, 14-4RD, 20-1OH) is not found to be associated with any known N-NW faults. This fracture trend might be controlled by local faults.

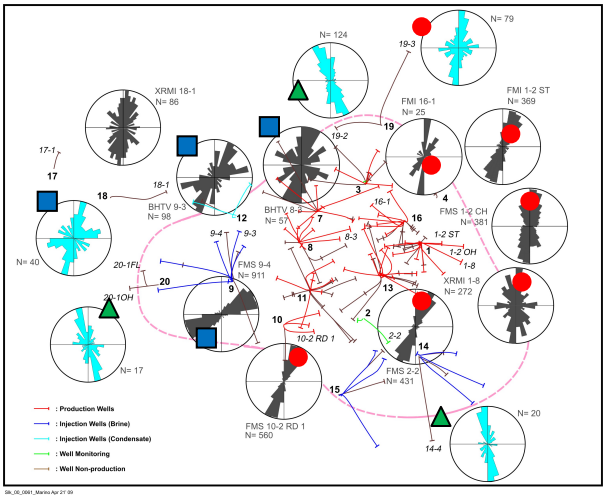

Figure 14: Map showing borehole image logs (FMS, FMI, XRMI) for Salak wells and rosettes showing the strike of open and partially open fractures. Red circles denote a strong N-NE fracture pattern, blue squares show a N-NE associated with E-W and NW striking fracture pattern, and green triangle shows wells with N-NW striking fracture pattern.

4. STRUCTURES AND THE CONCEPTUAL MODEL

Structural controls on the Salak reservoir are summarized in Figure 15. The upper figure shows a contour map of the reservoir top, which clearly displays that some major changes in the elevation of the reservoir top are related to faults. The conceptual cartoon stresses that hot fluid upflow (red circles) and leakage to surface from the reservoir are associated with major structures. Similarly, ingress of cooler marginal or overlying fluids recharge is locally controlled by major structures and their intersections.

The distribution of upflow and outflow shown is supported by initial well temperatures and pressures, and well as initial geochemical compositions (Stimac et al., 2008). Some of the inflows shown were identified in early studies, but others have only become apparent from monitoring of

well geochemical and enthalpy trends, and from repeat precision gravity surveys (Nordquist et al., 2010).

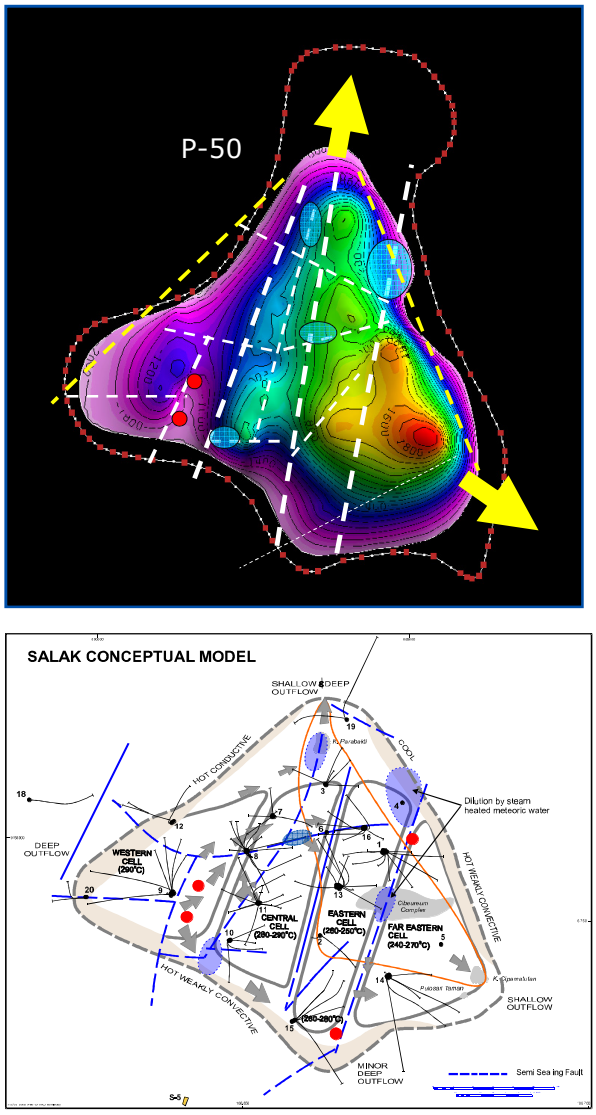

Figure 15: Map of Salak reservoir top (above) and cartoon of a simplified conceptual model for the Salak reservoir (below). Upflow is shown with red circles and direction of flow in reservoir at initial conditions is shown by gray arrows. Inflow of cooler inflows of marginal or overlying steam-heated waters is shown in blue.

ACKNOWLEDGEMENTS

The authors gratefully acknowledge Chevron for permission to publish this work. Image log interpretation on early Salak wells was done by Julie Shemeta. More recent interpretations were done by the authors, with assistance from Tony Dimabuyu and Halliburton staff. Running and processing of logs was also facilitated by staff of Halliburton and Schlumberger, as well as the Chevron Drilling Team and Apexindo Rig 4 staff.

REFERENCES

Acuña, J.A., Stimac, J., Sirad-Azwar, L., Pasikki, R.G.: Reservoir management at Awibengkok geothermal field, West Java, Indonesia. *Geothermics*, **37**, (2008), 332-346.

Hulen, J., Goff, F., Woldegabriel, G.: Hydrothermal Breccias in the Awi 1-2 Corehole, Awibengkok Geothermal Field, West Java, Indonesia. Geothermal Resources Council Transactions 23 (1999), 13-17.

Moore, J., Norman, D.: The Thermal and Chemical Evolution of the Hydrothermal Minerals in Awibengkok 1-2, Awibengkok Geothermal Field, West Java, Indonesia. Geothermal Resources Council Transactions 23 (1999), 25-29.

Nordquist, G.A., Acuña, J., and Stimac, J.A.: Precision Gravity Modeling and Interpretation – Awibengkok Field, Java Indonesia. Proceedings WGC2010, this volume (2010).

Stephenson, B.: Geologic map of the Gunung Salak Contract area, unpublished Unocal map (1985).

Stimac, J., Nordquist, G., Suminar, A., Sirad-Azwar, L.: An overview of the Awibengkok geothermal system, Indonesia, *Geothermics* **37**, (2008), 300-331.

Sugiaman, F.: State of stress and wellbore stability in Awibenkgok field. Unpublished Unocal report. (2003).

Yoshioka, K., Stimac, J.: Geologic and Geomechanical Reservoir Simulation Modeling of High Pressure Injection, West Salak, Indonesia. Proceedings WGC2010, this volume (2010).